Pergamon

0042-6989(94)00264-9

Vision Res. Vol. 35, No. 11, pp. 1547–1563, 1995

0042-6989/95 $9.50 + 0.00

Temporal and Chromatic Properties of Motion Mechanisms

KARL R. GEGENFURTNER,* MICHAEL J. HAWKEN†

Received 8 June 1994; in revised form 4 October 1994

We measured threshold contours in color space for detecting drifting sinusoidal gratings over a range of temporal frequencies, and for identifying their direction of motion. Observers were able to correctly identify the direction of motion in all directions of color space, given a sufficiently high contrast. At low temporal frequencies we found differences between luminance and isoluminance conditions; for isoluminance there was a marked threshold elevation for identification when compared to detection. The threshold elevation for identification is dependent on eccentricity as well as on temporal frequency. At high temporal frequencies there were no differences between detection and identification thresholds, or between thresholds for luminance and isoluminance. A quantitative analysis of the threshold contours allowed us to identify two mechanisms contributing to motion: a color-opponent mechanism with a high sensitivity at low temporal frequencies and a luminance mechanism whose relative sensitivity increases with temporal frequency. An analysis of the cone contributions to motion detection and identification showed that L-cones dominated threshold behavior for both detection and identification at high temporal frequencies. There was a weak S-cone input to motion detection and identification at high temporal frequencies.

Isoluminance Color Cones

INTRODUCTION

The idea that visual processing proceeds by the separate analysis of color, form and motion has received both physiological and psychophysical support (Zeki, 1978; Ramachandran & Gregory, 1978; Livingstone & Hubel, 1984, 1987). Separate analysis means that low level motion and color processing are initially distinct and independent. Furthermore, the luminance and color opponent mechanisms are believed to be responsible for motion and color analysis respectively. Isoluminant targets stimulate the color opponent pathway, but not the luminance pathway, so they are widely used to isolate color-opponent mechanisms. Psychophysical experiments have shown that the perception of visual motion is possible at isoluminance, even when potential luminance artifacts are carefully controlled (Lindsey & Teller, 1990; Cavanagh & Anstis, 1991; Mullen & Boulton, 1992). Moreover, several recent experiments showed that sensitivity for slowly drifting isoluminant gratings under foveal viewing conditions can even exceed that for luminance defined patterns, when the input to the visual system is expressed as the contrast in the three classes of cones (Stromeyer, Eskew & Kronauer, 1990; Stromeyer, Kronauer, Ryu, Chaparro & Eskew, 1995; Derrington & Henning, 1993; Mehta, Vingrys & Badcock, 1994). These psychophysical findings indicate that there is not a complete separation of motion and color. In addition, isoluminant stimuli produce a substantial motion aftereffect (Mullen & Baker, 1985; Cavanagh & Favreau, 1985; Derrington & Badcock, 1985) clearly indicating that there are conditions when color and motion can share a common pathway.

Nonetheless, there are clear differences between motion defined by luminance and isoluminant targets. Typically, isoluminant stimuli appear to move more slowly than luminance stimuli of identical speed and comparable contrast (Cavanagh, Tyler & Favreau, 1984; Mullen & Boulton, 1992). Detection thresholds for isoluminant patterns are lower than thresholds for identifying their direction of motion, even though this result does seem to depend on viewing conditions (Cavanagh & Anstis, 1991; Mullen & Boulton, 1992; Lindsey & Teller, 1990; Palmer, Mobley & Teller, 1993; Derrington & Henning, 1993; Mehta *et al.*, 1994).

The speed of target movement is a factor that has received relatively little consideration in many studies that have investigated the relative contributions of the luminance and chromatic pathways to motion. Nonetheless, recent physiological and clinical results (Merigan, Byrne & Maunsell, 1991; Hess, Baker & Zihl, 1989) indicate some separation in the anatomical pathways that process slow and fast moving patterns. In Merigan *et al.*'s (1991) experiments monkeys showed threshold elevations

*Max Planck Institute for Biological Cybernetics, Spemannstr. 38, 72076 Tübingen, Germany.
†Center for Neural Science, New York University, 4 Washington Place, New York, NY 10003, U.S.A.

for the detection of fast moving luminance patterns after magnocellular LGN lesions, but no threshold elevation for slowly moving luminance patterns. Hess *et al.* (1989) tested Zihl's patient (Zihl, Van Cramon & Mai, 1983), who suffers from a selective deficit of motion perception after bilateral damage to a circumscribed area of the posterior temporal cortex, with moving patterns of various drift rates. Motion processing at moderate to high speeds was impossible, but they found no deficits for slowly moving patterns.

A fast/slow dichotomy is also supported by a variety of psychophysical experiments (Thompson, 1982; Stone & Thompson, 1992; Gorea, Papathomas & Kovacs, 1993; Hawken, Gegenfurtner & Tang, 1994). Thompson (1982) and Stone and Thompson (1992) showed that the perceived speed of slowly moving luminance targets is contrast dependent while the perceived speed of fast moving targets is almost independent of contrast. Our recent psychophysical experiments comparing luminance and isoluminant targets using the Thompson paradigm showed significant differences in motion processing at slow and fast speeds (Hawken *et al.*, 1994). In particular, we found that perceived speed was contrast dependent for isoluminant targets at slow speeds, as it is for luminance targets (Thompson, 1982; Stone & Thompson, 1992), but that the velocity gain for isoluminant targets as a function of contrast is much higher than for luminance targets. At temporal frequencies higher than 4 Hz processing of motion is contrast independent for all stimuli, and isoluminant stimuli do not appear to be slowed down. We concluded that only a single pathway is required to account for the luminance and chromatic motion sensitivity at intermediate to high speeds while two pathways are required to account for motion sensitivity at low speeds. Gorea *et al.* (1993) show a similar distinction between the processing of slowly and fast moving targets. However, they conclude that there is a single mechanism for slowly moving luminance and colored patterns while there are dual fast pathways, one sensitive to luminance and the other sensitive to color.

The available evidence points to more than one motion mechanism. Using a quadrature-pedestal paradigm Stromeyer, Kronauer & Eskew (1992a) isolated two separate motion mechanisms. In their pedestal experiments the interaction between mechanisms is minimized so that each mechanism can be characterized in isolation. The interaction between mechanisms is not explicitly studied. We have taken a different approach. We have measured threshold contours in color space, over a wide range of temporal frequencies, in order to find the relative contributions of different mechanisms to target detection and to the identification of target motion. In the experiments described here we used conditions under which thresholds in different directions of color space were roughly equal. Therefore different mechanisms were active at the same time, and we could also study interactions between them. The shape of the contours allows us to assess if there are any systematic changes in the characteristics of mechanisms as a function temporal frequency. Preliminary reports of these results have been given in Gegenfurtner and Hawken (1992, 1993).

METHODS

Detection and identification in the fovea

Equipment. The stimuli were displayed on a BARCO calibrator CCID 7351B color television monitor driven by a custom-modified AT TrueVision graphics board which generates images on the monitor by reading through the picture memory in a raster scan and interpreting the numbers in each location as a color defined in a 256-element color lookup table. The intensity of each of the three primaries was controlled by two 8-bit digital-to-analog converters which gave a 14-bit resolution of the intensity. Lookup tables were used to linearize the relationship between voltage output and luminance for each phosphor. The display was refreshed at 128 Hz interlaced. All of the stimuli in the present experiments had a space-time averaged luminance of 33.7 cd m^{-2}.

Subjects. Data was collected from three experienced psychophysical observers (KG, MH and CT). One observer (CT) was naive with respect to the goals of the experiment. All observers had normal color-vision (as determined by Ishihara plates and the Farnsworth–Munsell 100-hue test) and normal or corrected-to-normal visual acuity. Full data sets were obtained for observers KG and CT, while observer MH only ran some of the conditions. The data from all three observers were in remarkable agreement with each other. Therefore we will present data from CT and KG only.

Stimuli. We measured thresholds for the detection of a sinewave grating, and for the identification of its direction of motion. The stimulus was a vertically oriented 1 c/deg sinewave grating displayed in a circular aperture with a diameter of 10 deg. The grating drifted within the window for a duration of 1 sec. Its contrast was multiplied by a Gaussian temporal envelope with a time constant of 250 msec. In the *identification* task, a fixation spot was displayed briefly, turned off, and followed by the presentation of the grating. The observer's task was to indicate whether the grating drifted rightward or leftward, by pressing either one of two buttons. In the *detection* task, there were two presentation intervals, each one marked by an audible burst of noise. In one of the two intervals the drifting grating was presented, in the other interval the uniform gray background. The observer had to indicate by a button press which one of the two intervals contained the grating. Subjects were seated at a distance of 167 cm away from the monitor, which subtended 12 × 12 deg of visual angle. The stimuli were presented on a uniform gray background of mean luminance, extending over the whole monitor screen. Stimuli in different directions of color space were interleaved in one session. Temporal frequency was held constant throughout one session. Thresholds for detection and identification were measured in separate sessions. A staircase procedure was used to measure the

threshold levels at which the grating could be detected or its direction of motion identified in 79% of the trials. Temporal frequency was varied between 1 and 16 Hz resulting in target velocities of 1–16 deg/sec.

Color space. The sinusoids were modulations symmetric around a central white point with C.I.E. xyY coordinates (0.326, 0.328, 33.7). We define three axes in color space: a red–green axis from red (0.397, 0.292, 33.7) to green (0.237, 0.372, 33.7); an S-cone isolating blue–yellow axis from purplish blue (0.286, 0.241, 33.7) to yellow (0.409, 0.508, 33.7); and a luminance axis from black to white. These axes differentially excite the putative second stage color-opponent mechanisms identified by Krauskopf *et al.* (Krauskopf, Williams & Heeley, 1982; Derrington, Krauskopf & Lennie, 1984). The C.I.E. coordinates of the stimuli were transformed into cone excitations using the primaries measured by Smith and Pokorny (1975).

Detection and identification in the parafovea

In the second experiment we measured analogous thresholds for stimuli presented in the perifovea (1 deg) and the parafovea (4 deg). The major difference was a smaller stimulus size and a shorter presentation interval to minimize eye movements. We used similar procedures as in the first experiment, with the following exceptions. A regular AT-Vista board with 8-bit digital-to-analog converters was used. To obtain a higher precision in the control of color we interleaved stimulus frames with a frame of uniform grey mean luminance. This effectively doubled the chromatic resolution to 9 bits while reducing the temporal resolution to 64 Hz. Detection and identification thresholds were measured at the same time using a two-alternative forced-choice procedure. The stimulus was a vertically oriented 1 c/deg sinewave grating vignetted by a two-dimensional Gaussian window with a standard deviation of 1 deg. At the beginning of each trial a fixation spot was displayed briefly, followed by the presentation of the grating, which was drifting within the window for a duration of 250 msec. The observer had to make two button presses indicating whether the grating appeared to the right or to the left of the fixation spot (the detection task), and whether the grating moved to the right or to the left (the identification task). The location of the center of the Gaussian window was either 1 deg away from the fixation spot, or at an eccentricity of 4 deg. We ran preliminary experiments in several directions of color space to determine approximate threshold contrast levels. We then used a method of constant stimuli and fitted a psychometric function to the resulting choice proportions to obtain exact threshold estimates.

RESULTS

Detection and identification in the fovea

Initially we examine the effects of varying L- and M-cone modulations on motion detection and identification. We start by explaining the typical data format, which is shown in most subsequent graphs. Figure 1 shows data from subject KG for a grating with a temporal frequency of 4 Hz. The L-cone contrast is shown on the x-axis; stimuli along this axis consist of bright-red and dark-green grating bars. M-cone contrast is shown on the y-axis; stimuli along this axis consist of dark-red and bright-green grating bars. The solid diagonal lines through the origin show the luminance and the isoluminance directions, as defined by the human photometric luminance sensitivity curve $V(\lambda)$. Along the positive diagonal L- and M-cone excitation covaries. Lines with a slope of -2 indicate a constant photometric luminance. The open symbols denote detection threshold and the solid symbols are for identification. Because the stimuli are symmetrical modulations around the origin, stimuli reflected through the origin are physically identical. Therefore we also plotted each data point twice. Data points corresponding to negative contrast values are simply reflected through the origin. The graph is typical in many respects. For points in the luminance direction thresholds for detection and identification of the direction of motion are equal, as previous investigators have found (Watson, Thompson, Murphy & Nachmias, 1980). For points on the isoluminant line thresholds for detection are slightly, but consistently lower than for identification, as reported by other investigators (Cavanagh & Anstis, 1991; Mullen & Boulton, 1992; Lindsey & Teller, 1990; Palmer *et al.*, 1993).

Figure 2 shows threshold contours for subject CT at six different temporal frequencies, ranging from 1 to 16 Hz. Figure 3(A–C) shows threshold contours for subject KG at three different temporal frequencies in the same range. They follow the format detailed in Fig. 1. These data exemplify three major findings:

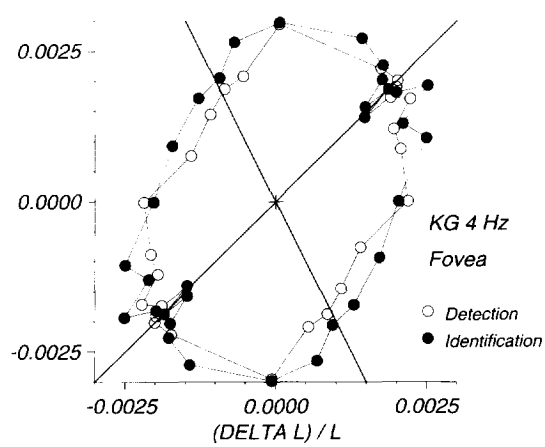

FIGURE 1. Threshold contours for subject KG for the detection (open symbols) and identification of the direction of motion (solid symbols) of a foveally presented grating with a temporal frequency of 4 Hz. Because of the symmetry of the stimuli around the origin each data point is drawn twice, once reflected around the origin. On the horizontal axis the contrast of the L-cones is plotted, on the vertical axis the contrast of the M-cones. The solid lines through the origin indicate the directions in which luminance was kept constant (isoluminance, negative slope) and in which stimuli had no chromatic component (luminance, positive diagonal).

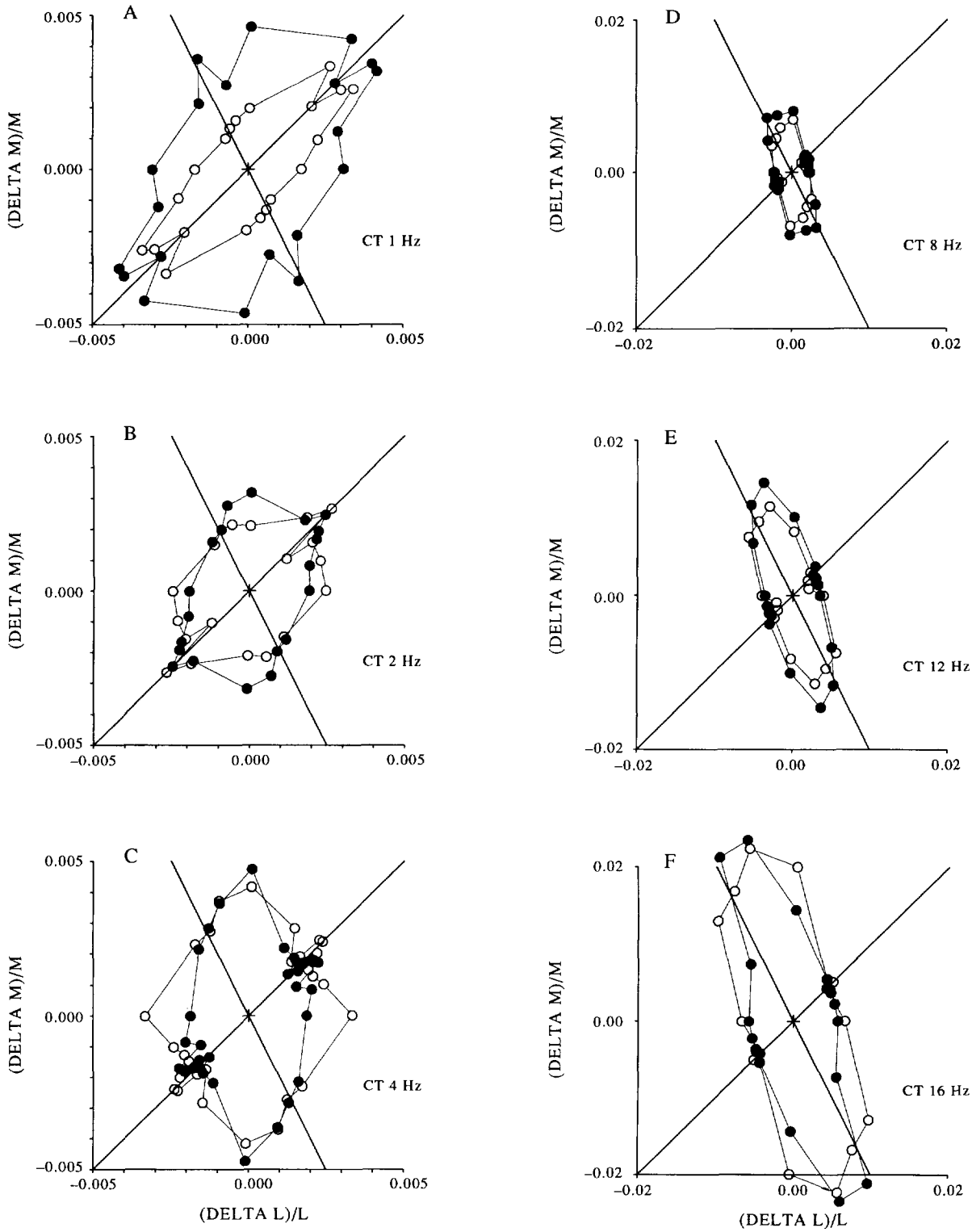

FIGURE 2. Threshold contours for subject CT for a 1 c/deg foveally presented grating drifting at temporal frequencies of (A) 1 Hz, (B) 2 Hz, (C) 4 Hz, (D) 8 Hz, (E) 12 Hz, (F) 16 Hz. Notice the different scale in (A)–(C) and (D)–(F). All other details as in Fig. 1.

(1) Observers are able to report the direction of motion for all the combinations of color and temporal frequency that were tested. Even at isoluminance clearly defined identification thresholds were obtained for all three observers indicating that the motion system is sensitive to color across all temporal frequencies.

(2) For slowly drifting stimuli (1 Hz) the most consistent and reliable differences between detection and identification thresholds occur when the color direction is at or near photometric isoluminance [Figs 2(A) and 3(A)]. Both subjects show elevations in identification threshold near to isoluminance although it

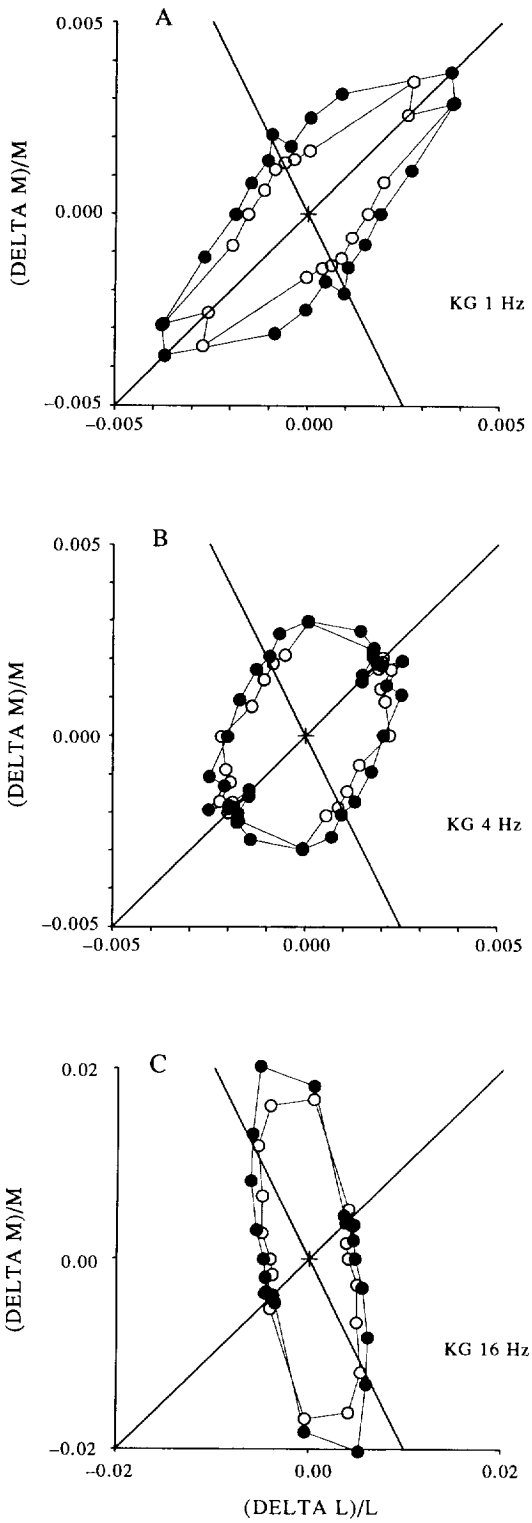

FIGURE 3. Threshold contours for subject KG for foveally presented gratings drifting at temporal frequencies of (A) 1 Hz, (B) 4 Hz and (C) 16 Hz. All other details as in Fig. 1.

is clear that the absolute elevation differs between subjects.

(3) There is a change in the orientation of the principal axes of both detection and identification contours as a function of temporal frequency [Figs 2(A, C, F) and 3(A, B, C)] with a transition point at around 4 Hz. The relative sensitivity in the luminance direction increases compared to the isoluminance direction.

The contours show that when thresholds are expressed in the cone contrast metric, they are lowest for slowly moving isoluminant stimuli. This has been emphasized recently by Stromeyer *et al.* (1990). Systematic differences between detection and identification occur only for slowly drifting isoluminant stimuli below 2 Hz. At higher temporal frequencies there is no difference between detection and identification threshold. Thresholds in the isoluminant direction are actually lowest at the lowest temporal frequencies, and increase steadily. For luminance the thresholds reach a minimum at around 4 Hz [Figs 2(C) and 3(B)], and increase for lower and higher temporal frequencies. At temporal frequencies of 8 Hz and above [Figs 2(D–F) and 3(C)] the shape of the threshold contour does not appear to change any more. There is simply an overall increase in the magnitude of thresholds. At the highest temporal frequencies [Figs 2(D–F) and 3(C)] there is an indication that threshold stimuli in some directions (M-cone only) might require more luminance contrast for detection or identification than the luminance stimulus (positive diagonal). We will investigate these aspects of the data quantitatively below. Finally, the contours for the two observers and the ones for observer MH, which were not shown here, agree in all respects.

S-cone contributions to motion

In the above experiments we have concentrated on the contributions of the L- and M-cones to motion. Figure 4 shows data for subject KG for stimuli in a different plane of color space, spanned by luminance and the S-cone isolating direction. On the y-axis luminance is varied by covarying L- and M-cone inputs. On the x-axis the S-cone contrast varies. It should be noted that the scale on the S-cone axis is 10 times greater than that of the luminance axis. The difference in scale makes the contours for the 1 and 4 Hz conditions appear roughly circular around the midpoint when, in fact, the thresholds in the S-cone direction are larger by an order of magnitude. At 16 Hz [Fig. 4(C)], for example, an S-cone contrast as high as 10% is required at threshold. For slow movement [1 Hz, Fig. 4(A)], as with red–green isoluminant stimuli, thresholds are greater for identification than for detection in the isoluminant blue–yellow direction. Once again, this difference between detection and identification thresholds disappears at higher temporal frequencies. Even more noticeable is the change in the orientation of the principal axis of the threshold contour at 16 Hz. The largest thresholds do not occur in the S-cone isolating direction, but in a direction where the magnitude of S-cone modulation is negatively correlated with the magnitude of luminance modulation. This indicates that at the high temporal frequencies the S-cones do contribute to motion. However, the magnitude of the contribution is rather small (remember the different scale of the axes). This confirms a result by Lee and Stromeyer (1989), but at a significantly lower illuminance than they had used.

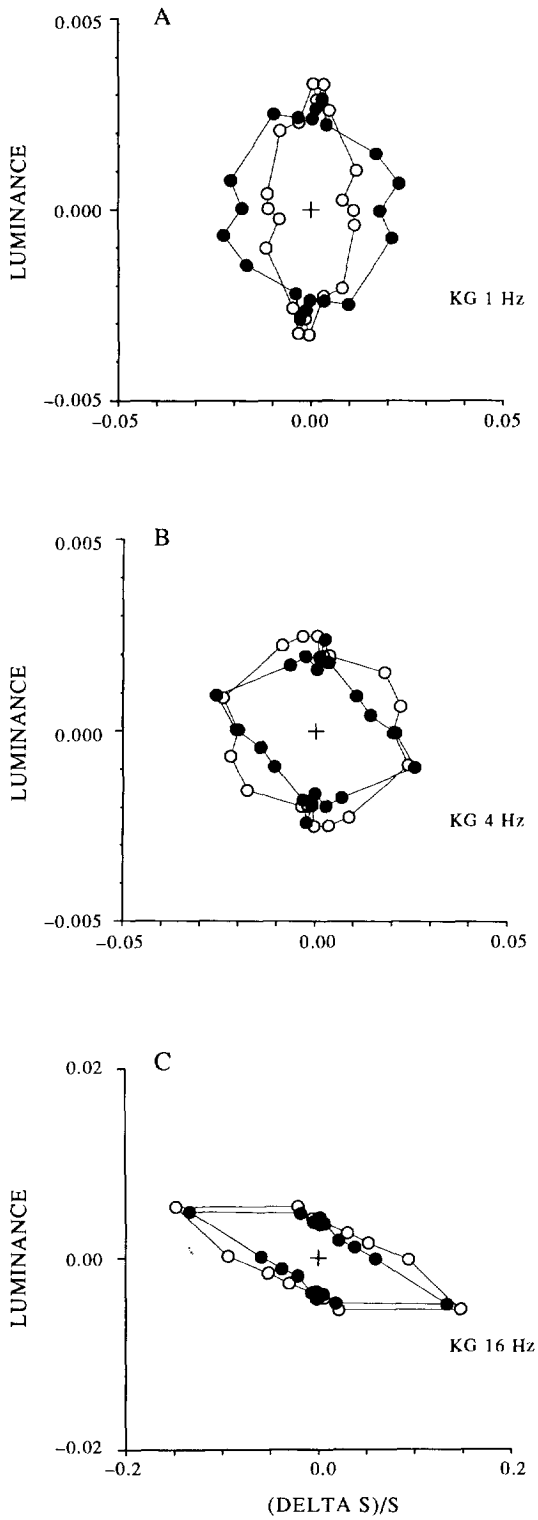

FIGURE 4. Threshold contours for subject KG for stimuli in a plane spanned by luminance and S cones. The x-axis plots S-cone contrast. The y-axis shows luminance contrast (with equal L- and M-cone contrast). Data are for gratings drifting at temporal frequencies of (A) 1 Hz, (B) 4 Hz and (C) 16 Hz. Note that the x-axis scale is an order of magnitude greater than the y-axis scale.

Modulation of stimuli in the photometric isoluminant plane allows us to compare S-cone contributions to motion with the contributions of a red–green color-opponent mechanism. Figure 5 shows data for subject KG for stimuli modulated in the photometric isoluminant plane. As in the previous figure the values for S-cone contrast (y-axis) are 10 times the values for the L-cone

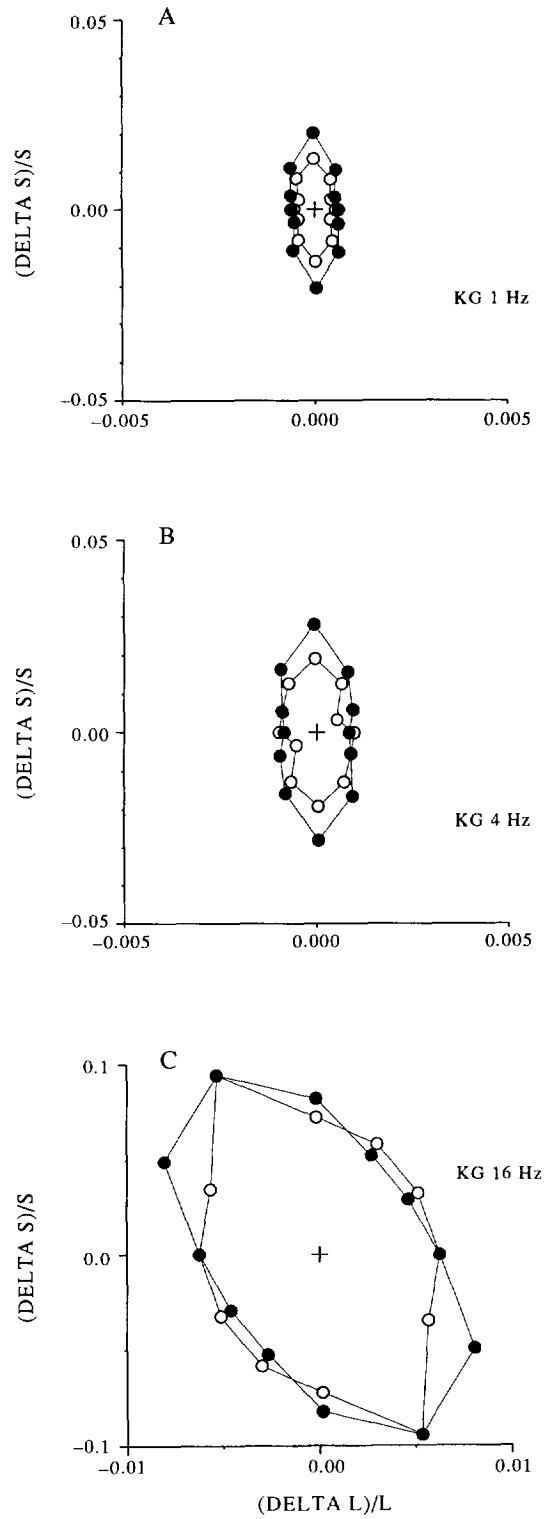

FIGURE 5. Threshold contours for subject KG for stimuli in the photometric isoluminant plane. The axes of the diagram correspond to the axes of the chromaticity diagram introduced by MacLeod and Boynton (1979). The x-axis plots L-cone contrast (inversely proportional to M-cone contrast), the y-axis S-cone contrast. Data are for gratings drifting at temporal frequencies of (A) 1 Hz, (B) 4 Hz and (C) 16 Hz. Note that the y-axis scale is an order of magnitude greater than the x-axis scale.

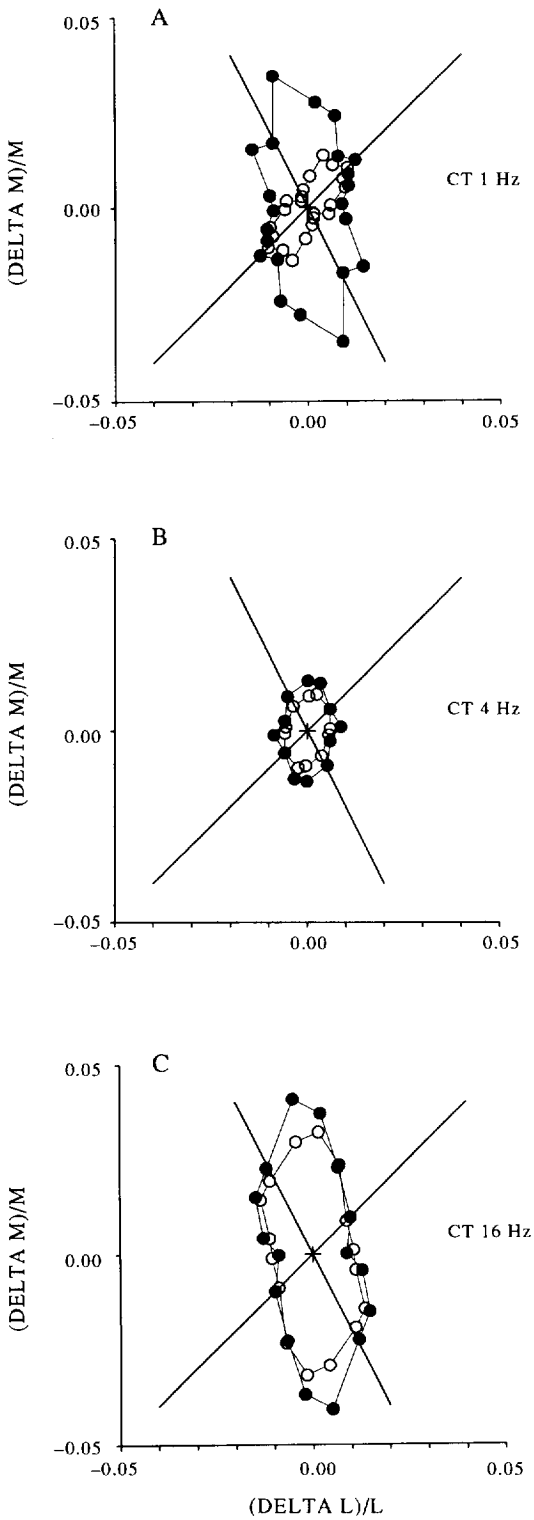

FIGURE 6. Threshold contours for subject CT for gratings presented perifoveally. The x-axis plots L-cone contrast, the y-axis M-cone contrast. Gratings were drifting at temporal frequencies of (A) 1 Hz, (B) 4 Hz and (C) 16 Hz. All other details as in Fig. 1.

contrast (x-axis). Thresholds for both detection and identification are greatest in the S-cone direction and the differences between detection and identification are maximal in the S-cone direction for low and intermediate temporal frequencies. However, even in the S-cone isolating direction the motion of the pattern is eventually seen, if the contrast is high enough (2.5% S-cone contrast). From 1 Hz [Fig. 5(A)] to 4 Hz [Fig, 5(B)] there is a scaled increase in thresholds. At 16 Hz [Fig. 5(C)] the largest thresholds are along the negative diagonal, the direction where S- and L-cone modulation are negatively correlated, just as before in Fig. 4(C). This provides further evidence that S-cones do contribute to motion at high temporal frequencies.

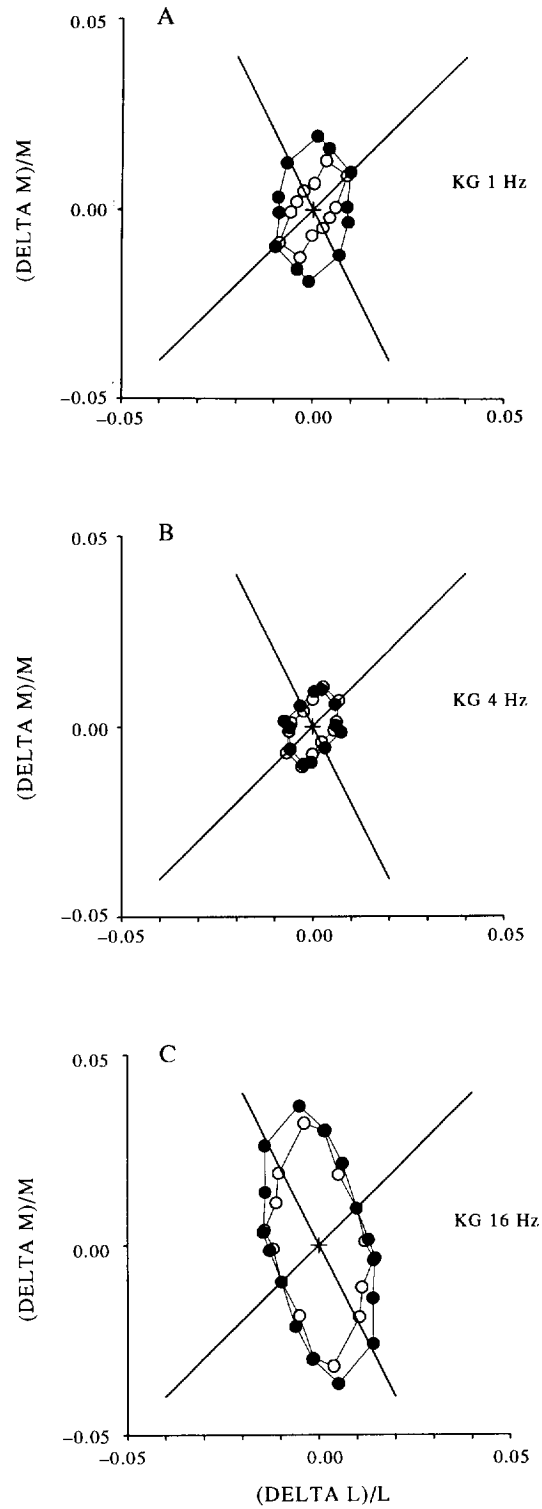

FIGURE 7. Threshold contours for subject KG for gratings presented perifoveally. The x-axis plots L-cone contrast, the y-axis M-cone contrast. Gratings were drifting at temporal frequencies of (A) 1 Hz, (B) 4 Hz and (C) 16 Hz. All other details as in Fig. 1.

In summary, we have shown that under large field foveal viewing conditions the direction of motion can be seen in all directions of color space we tested, given a high enough input contrast.

Detection and identification in the parafovea

The difference between detection and identification thresholds for isoluminant stimuli depends to some extent on eccentricity (Cavanagh & Anstis, 1991; Mullen & Boulton, 1992; Lindsey & Teller, 1990; Palmer *et al.*, 1993; Derrington & Henning, 1993). In order to determine whether there is a systematic influence of eccentricity we measured detection and identification threshold contours for small Gabor patches of drifting grating at 1 and 4 deg eccentric to the observers fixation point. Figure 6 shows detection and identification contours measured in the perifovea (1 deg) for subject CT at three temporal frequencies: 1, 4 and 16 Hz. Figure 7 shows data for the same set of conditions for subject KG. Compared to the foveal condition there is a large increase in overall threshold magnitude. To some degree the threshold elevation can be attributed to the shorter presentation time (250 msec) and the smaller stimulus size (1 deg Gaussian space constant) for the perifoveal condition. However, the main point of interest is the difference in detection and identification thresholds. For observer CT, the slowly drifting isoluminant stimuli in the perifovea [Fig. 6(A)] show a very substantial elevation in threshold for identification, about 5 times that of detection. This can be compared with the foveal condition for the same observer [Fig. 2(A)] where the sensitivity ratio of detection to identification is about 2. For observer KG the detection/identification sensitivity ratio is somewhat smaller than for CT in the perifovea at 1 Hz [Fig. 7(A)] but it is clearly a more substantial elevation than in the corresponding foveal condition [Fig. 3(A)]. As before, there is no difference between detection and identification for stimuli modulated in or near the luminance direction [positive diagonals in Figs 6(A) and 7(A)]. At higher temporal frequencies the contours show a similar pattern to the foveal data, where the detection and identification contours are the same shape, and the principal axis tends towards the L-cone at the highest temporal frequencies. Contours of the two observers for the 4 and 16 Hz conditions are remarkably similar [cf. Fig. 6(B, C) with Fig. 7(B, C)].

When detection and identification thresholds are measured in the parafovea [Figs 8(A–C) and 9(A–C)], there are significant changes in the detection to identification ratio when compared to foveal and perifoveal conditions. For both subjects at 1 Hz there is a more pronounced differentiation between the detection and identification thresholds. There is only one color direction, the luminance direction, where motion is identified at detection threshold [Figs 8(A) and 9(A)]. At all other points more contrast is required for the subject to identify the direction of motion. The difference between detection and identification threshold at or near isoluminance persists when the temporal frequency is raised to 4 Hz. In the foveal and perifoveal conditions there is no such elevation at 4 Hz. Nonetheless, by 16 Hz both detection and identification contours have attained the same shape, and are indistinguishable between subjects and across eccentricity.

The 4 Hz condition for both observers [Figs 8(B) and 9(B)] illustrates that the shape of the detection and identification contours are fundamentally different. The detection contour (open circles) forms a parallelogram, the identification contour (solid circles) can be fitted well by an ellipse. If we assume that two mechanisms underlie the threshold contour, then an elliptical threshold contour indicates probability summation. A parallelogram indicates no summation. Because of these apparent differences, we describe a quantitative analysis of the threshold contours in the following section.

Identification of mechanisms

There are a number of our detection and identification contours that have many points falling close to a line parallel to the luminance or the isoluminance direction. When thresholds lie exactly on a line it could be inferred that the stimuli are detected by a single linear mechanism. For example in the experiment summarized in Figs 8(B) and 9(B) the two mechanisms would be either a "luminance" or a "color-opponent" mechanism. However, as shown by Nielson and Wandell (1988) and by Poirson, Wandell, Varner and Brainard (1990), the identification of individual mechanisms is crucially dependent on the exact shape of the contours. Under the assumptions of their model, fitting an ellipse to a threshold contour does not allow the identification of the low-level mechanisms underlying perception. We sought to test whether there are identifiable low-level mechanisms underlying our contours by fitting both ellipses and parallelograms. There are two aspects of the mechanisms that we have concentrated on here: (1) whether the contours across all temporal frequencies could be adequately accounted for by two mechanisms, identifiable as a "luminance" and a "color opponent" mechanism; and (2) whether these mechanisms have constant chromatic properties across all temporal frequencies.

In our fitting procedure we followed the methods outlined by Poirson *et al.* (1990). Briefly, threshold vectors $\mathbf{x}_i$ are transformed by a linear transformation denoted by a matrix A from stimulus space into a space where the length of all threshold vectors equals 1. We will call the transformed vectors $\mathbf{m}_i$, where i is the index for the direction in color space:

$$\mathbf{m}_i = A\mathbf{x}_i. \quad (1)$$

The ellipse is transformed into a circle. If all the data points do indeed lie on an ellipse in stimulus space, then they will lie on a unit circle in the transformed space. In our case, the stimulus space is the color space spanned by the contrasts in the L- and M-cones. We will ignore the S-cones in this part of the analysis since we have shown their contributions to be negligibly small. Each vector $\mathbf{x}_i$ will then contain as its two elements the contrast in the L- and M-cones at the threshold for color direction i, and A

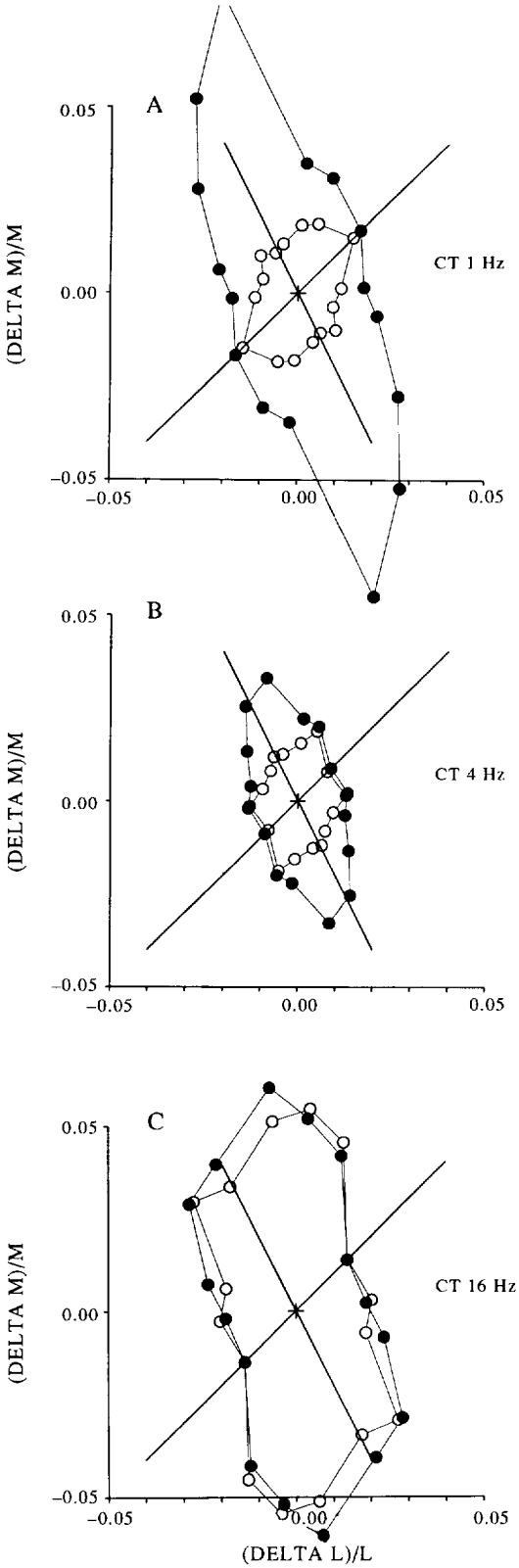

FIGURE 8. Threshold contours for subject CT for gratings presented parafoveally. The x-axis plots L-cone contrast, the y-axis M-cone contrast. Gratings were drifting at temporal frequencies of (A) 1 Hz, (B) 4 Hz and (C) 16 Hz. All other details as in Fig. 1.

is a 2×2 matrix. Deviations are then measured as the squared deviations of the transformed threshold vectors from unity:

$$\mathrm{err}_i = (1 - \|(A\mathbf{x}_i)^{\mathrm{T}}(A\mathbf{x}_i)\|)^2 = (1 - |\mathbf{m}_i^{\mathrm{T}}\,\mathbf{m}_i\|)^2. \quad (2)$$

This error measure is coordinate free in the sense that we will obtain the same fit independently of linear transformations of the stimulus space. A different choice of color space would not change the results. It is tempting to interpret the matrix A in terms of visual mechanisms, since it specifies how the cone inputs are scaled and weighted. However, it can also be seen from equation (2)

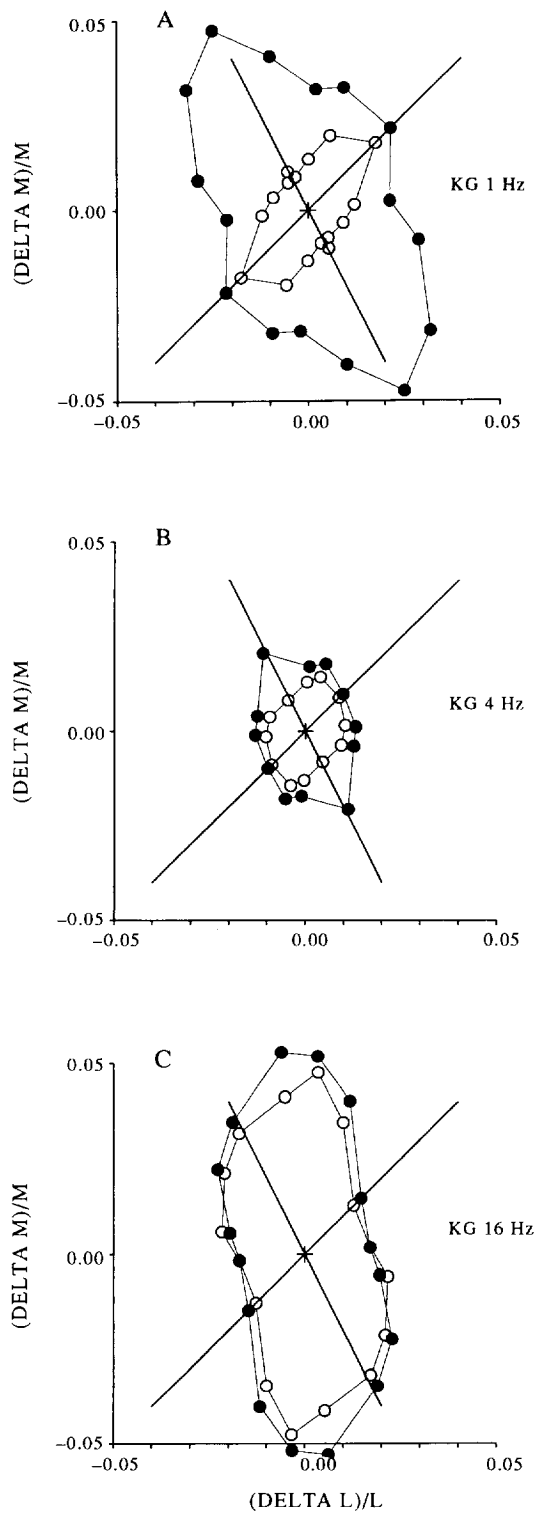

FIGURE 9. Threshold contours for subject KG for gratings presented parafoveally. The x-axis plots L-cone contrast, the y-axis M-cone contrast. Gratings were drifting at temporal frequencies of (A) 1 Hz, (B) 4 Hz and (C) 16 Hz. All other details as in Fig. 1.

that the fit will not change if we multiply the best fitting matrix A with an orthogonal matrix, one that does not change vector length, since $(OA)^T(OA)$ is equal to A^TO^TOA, which in turn reduces to A^TA for any orthogonal matrix O. Therefore we cannot conclude anything about visual mechanisms from knowledge of the matrix A. For example, the detection threshold contours in Figs 2(A) and 3(A) seem to indicate the activity of a color-opponent mechanism, since most data points fall close to a line parallel to the luminance direction in color space. An ellipse fit with a matrix A giving equal weights of opposite signs to L- and M-cone inputs leads to a good fit of the data, because a line cannot be readily distinguished from an elongated ellipse. But because of equation (2) we are permitted to change matrix A by rotation, which arbitrarily changes the cone weights. This makes an interpretation in terms of cone weights impossible. Therefore, we cannot conclude from Figs 2(A) or 3(A) that the visual mechanism underlying detection is color-opponent.

If we can show that the ellipse fit is inadequate and that the threshold contours can be fitted by parallelograms adequately, we do get a unique characterization of the underlying visual mechanisms. In that case we also estimate a linear transformation A which transforms the threshold vectors. But this time we minimize instead:

$$\mathrm{err}_i = (1 - \mathrm{MAX}_j(\mathbf{m}_{ij}))^2, \qquad (3)$$

where j runs over all stimulus dimensions. This allows a unique identification of mechanisms if the data can be described by parallelograms. Upon visual inspection some of the threshold contours seemed to be fitted better by parallelograms [Figs 8(B) and 9(B)]. If the parallelogram model indeed significantly improves the fit over the ellipse model we could obtain a characterization of the motion mechanisms, and the way they combine cone inputs.

In order to compare the efficacy of the ellipses and the parallelograms we computed the goodness of fit to all individual contours. The r.m.s. error for both ellipses and parallelograms is typically of the order of 10% in the transformed space, with little difference between subjects. The parallelogram fit is slightly better in most cases, but that is not surprising since the number of parameters is also larger. There are four free parameters in the matrix A for the parallelogram, compared to three for the ellipses. For all 36 conditions (3 eccentricities, 6 temporal frequencies, detection and identification) and two subjects (resulting in approx. 700 thresholds) with complete data sets the r.m.s. error was 10.5% for ellipses and 9.7% for parallelograms. We cannot reasonably discriminate between the two models. Figure 10(A) shows the worst fit for any of the 72 threshold contours: detection for subject CT in the perifovea [contour shown by open circles in Fig. 6(A)]. The r.m.s. error is 24% for the ellipse and 20% for the parallelogram. Even for this case the deviations of the models in cone contrast space are quite small. In all other cases the fits were markedly better.

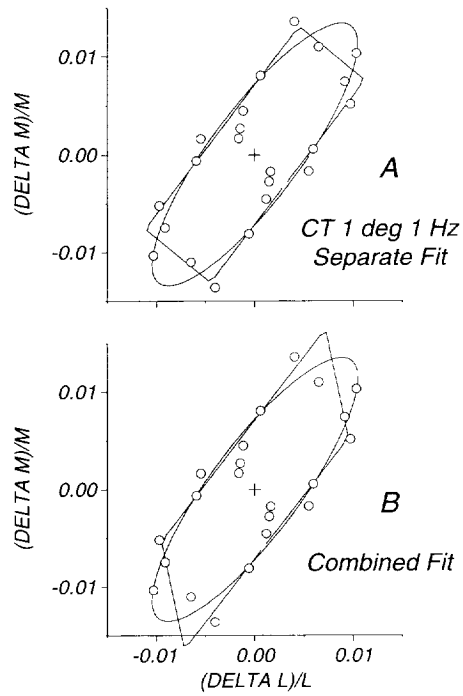

FIGURE 10. (A) The worst individual fit for the case in which models were fit separately to each threshold contour. Data are for detection of a 1 Hz grating at an eccentricity of 1 deg for subject CT. The r.m.s. error was 24% for the ellipse fit and 20% for the parallelogram fit. (B) The same fit for the case in which only one set of mechanisms was fit across all temporal frequencies. The r.m.s. error remained at 24% for the ellipse fit and increased to 21% for the parallelogram fit.

The similarity between the ellipse and parallelogram fits did not come as a big surprise. Poirson *et al.* (1990) have shown for other threshold contours that these two models are hard to discriminate between, as long as individual threshold contours are fitted. Recently, Maloney and Knoblauch (1994) suggested a way to discriminate the models based on the residual errors. They also pointed out the great difficulty of identifying mechanisms based on a single detection or discrimination contour. We adopted an alternative and more straightforward means of obtaining a unique characterization of mechanisms. If the chromatic properties of motion mechanisms, ie the way they combine cone inputs, do not change with temporal frequency, we can identify these mechanisms by fitting all contours simultaneously.

In the fits of the parallelogram model the sides of the parallelograms had similar orientations at different temporal frequencies. They were in the directions of luminance and isoluminance projections in color space. Only the distances from the origin varied. The major and minor axes of the ellipses deviated markedly from those of the parallelograms in cases where the sides of the parallelograms were nearly equal. A clear example of the inappropriateness of the ellipse fit was found when trying to accommodate detection contours in the parafovea at moderate temporal frequencies, which have a clear parallelogram shape [Fig. 9(B), detection]. The ambiguity in the ellipse fits prompted us to try a combined fit of all data sets. For the combined fit we assumed that only two mechanisms underlie all threshold contours, with chromatic properties that remain constant across

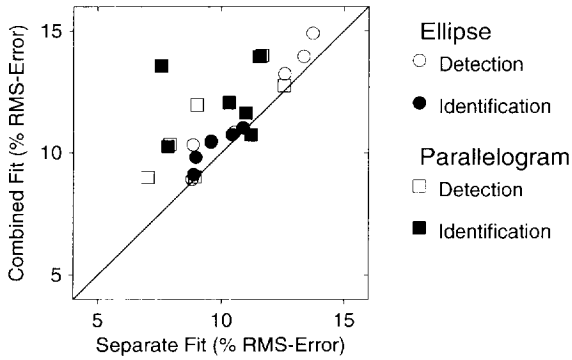

FIGURE 11. Quality of fits for the different models. Circles indicate ellipses, squares indicate parallelograms. Open symbols are for detection, solid symbols for identification. The r.m.s. errors, were computed across temporal frequencies and are shown for two subjects (KG and CT) and three different viewing conditions (fovea, 1 deg, 4 deg). The x-axis plots r.m.s. error for the case where the models were fitted individually to each threshold contour. The y-axis plots r.m.s. error for the case where only one set of mechanisms was estimated for all temporal frequencies.

temporal frequency. In the combined fits only the sensitivities of the mechanisms were allowed to change with temporal frequency. These hypothetical mechanisms were fit by an ellipse, or by a parallelogram. Then individual threshold contours were fit by scaling the sensitivity of each mechanism by a factor depending only on temporal frequency. In other words, for each threshold contour k we compute

$$\mathrm{err}_{ki} = (1 - \|(D_k A \mathbf{x}_i)^{\mathrm{T}}(D_k A \mathbf{x}_i)\|)^2, \qquad (4)$$

where the D_k are diagonal 2×2 matrices. All threshold contours are simultaneously transformed into a "mechanism" space, and D_k simply scales the sensitivities of the two mechanisms for that particular temporal frequency k. In this case the matrix A is completely determined both for the ellipse model and the parallelogram model, and the number of free parameters is the same in both fits (four parameters for the initial contour, and two per contour for all others).

The effect of that procedure on the worst-case fit from above is shown in Fig. 10(B). There is hardly any change in the quality of these particular fits. The r.m.s. error remains at 24% for the ellipse, whereas the fit for the parallelogram gets slightly worse (r.m.s. error increases from 20% to 21%). Figure 11 plots errors for both separate and combined fits, r.m.s. errors are shown for each condition (foveal, perifoveal and parafoveal) and for both observers (CT and KG). In case of the separate fits they were averaged across temporal frequencies. In most cases the fits are close to the diagonal, indicating that the combined fit is not much worse than the separate fits. Because the number of parameters in the combined fit is significantly reduced compared to the separate fits, it is the preferred one. For example, for the parallelogram fit we have 14 parameters now for the contours from 6 temporal frequencies (4 for the mechanism and 5×2 for the sensitivities) instead of 24 (6×4 mechanisms). However, we will see later on that there are systematic deviations for the combined fits.

Because the matrix A is uniquely determined in the combined fits we can interpret its elements in terms of visual mechanisms. Each element of the matrix A specifies how much each cone type gets weighted by the two different motion mechanisms. The elements of the matrix D specify the sensitivity of each mechanism at each temporal frequency. The particular mechanisms we found correspond to the ones we had expected. Furthermore, the mechanisms and sensitivities based on parallelogram and ellipse fits were virtually identical. One mechanism had weights of unequal sign for the L- and M-cones, and was therefore red–green color-opponent. The other mechanism had equal signs for both cone types, and was therefore a luminance mechanism. The sensitivities of the color-opponent mechanism were low-pass in temporal frequency, while the luminance mechanism was band-pass. These two mechanisms are similar to those that would be expected based on previous investigations. The cone weights for the color-opponent mechanism were roughly equal. This is expected because threshold contours at low temporal frequencies are aligned with the luminance direction. The exact weights were slightly in favor of the L-cones. We observed ratios of L- vs M-cone weights in the range of 1.2–1.5, with no systematic variation between eccentricity or subject. For the luminance mechanism we would expect a ratio of 2:1 for the L- and M-cones which equals photometric luminance as defined by $V(\lambda)$. However, our estimates gave ratios between 3:1 and 5:1, which is significantly higher than the $V(\lambda)$ value. Figure 10, for example, shows that the contour for the luminance mechanism is much steeper in the combined fit [Fig. 10(B), L:M = 5:1] than in the separate fits [Fig. 10(A), L:M = 0.9:1] at low temporal frequencies. Inspection of the contours for high temporal frequencies shows why this is the case. At high temporal frequencies the slope of the contours did indeed get steeper. At the low temporal frequencies the slope of the contour is not very well-defined, because only few data points fall on that part of the contour due to the relatively low sensitivity. With increasing temporal frequency contours of the luminance mechanism did get steeper. The results of the separate parallelogram fits indicated average ratios of about 2:1 at low temporal frequencies and ratios between 5:1 and 12:1 (subject KG, foveal condition, 16 Hz) at the highest temporal frequencies. Because the luminance mechanism was more sensitive than the color-opponent mechanism at high temporal frequencies, the estimated slope for the combined fit was relatively steep.

The temporal frequency dependence of the slope of the luminance contour constitutes a systematic deviation from the prediction of the combined fits. It means that the chromatic properties of motion mechanisms were not completely separable from the temporal properties. The relative weights for the L- and M-cones change as temporal frequency varies. However, the separate parallelogram fits indicated one color-opponent mechanism and one luminance mechanism at each temporal frequency. Whereas the weights for the color-opponent mechanism were relatively stable, only the weights for the

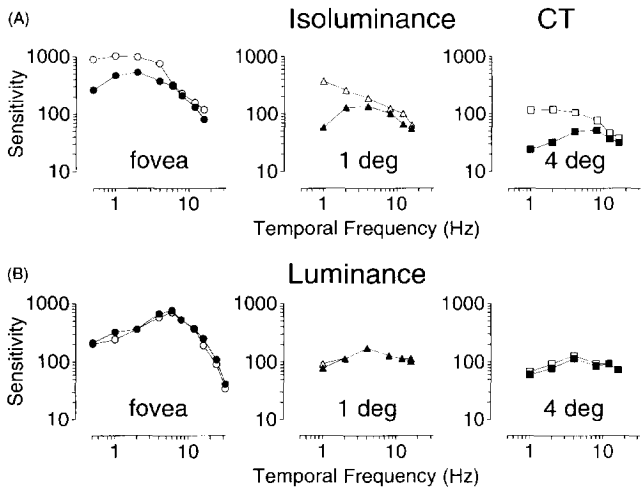

FIGURE 12. Cone contrast sensitivity for the detection (open symbols) and identification of direction of motion (solid symbols) of a 1 c/deg sinewave grating for subject CT. Left graphs are for the foveal, large field condition, middle graphs for the perifoveal condition (eccentricity 1 deg), and right graphs for the parafoveal condition (eccentricity 4 deg). (A) Isoluminance; (B) luminance. Cone contrast sensitivity is the reciprocal of the r.m.s. contrast of the L- and M-cones. For luminance it is the same as the reciprocal of Michelson contrast.

luminance mechanism gradually changed with temporal frequency.

Detection vs identification

We looked more closely at the sensitivity of the mechanisms indicated by the above analysis as a function of temporal frequency. In this and all the following graphs isoluminance will refer to the photometric isoluminance condition, as defined by the human photometric luminance sensitivity curve $V(\lambda)$, even if the largest threshold was sometimes in a direction slightly tilted away from photometric isoluminance. These deviations, it turned out, were not very large. Similarly, we will refer to the photometric luminance direction [$V(\lambda)$] as luminance, despite the above mentioned deviations at high temporal frequencies. Figures 12 and 13 summarize detection and identification at each of the three eccentricities to isoluminance (A) and luminance (B) stimuli, as a function of temporal frequency. For the foveal viewing condition (left graph), thresholds were measured in new experiments. In each session one color direction was used, and different temporal frequencies were interleaved. For the other conditions the data from Expt 2 are replotted. Chromatic sensitivity is specified as the reciprocal of r.m.s. contrast of the L- and M-cones. For the luminance condition [Figs 12(B) and 13(B)] detection and identification thresholds coincide at all temporal frequencies and for all eccentricities. At isoluminance [Figs 12(A) and 13(A)] over the lower temporal frequency range the sensitivity for the identification of motion (solid symbols) is consistently lower than the sensitivity for detection (open symbols). The difference in sensitivity between detection and identification gradually decreases as temporal frequency increases. There is also an effect of eccentricity: in the fovea sensitivity for motion identification becomes equal to sensitivity for detection at lower temporal frequencies than in the peri- or parafovea. These differences in detection and identification are mainly due to two factors, a decrease of identification performance at low temporal frequencies and, under foveal and perifoveal conditions, an increase in detection performance.

A wide range of motion detection to identification sensitivity ratios have been reported (Cavanagh & Anstis, 1991; Mullen & Boulton, 1992; Lindsey & Teller, 1990; Palmer *et al.*, 1993; Derrington & Henning, 1993). None of these studies systematically investigated the effect of temporal frequency. Ratios of detection vs identification sensitivities are shown in Figs 14 and 15 for the two observers CT and KG. For the luminance condition [Figs 14(A) and 15(A)] there was no elevation of identification threshold at any temporal frequency or at any of the three eccentricities tested. On the other hand, at isoluminance [Figs 14 and 15(B)], the detection/identification ratio approached a value of 5 for the parafoveal condition (squares) and decreased to unity as temporal frequency increased. In the fovea the ratio was lower but showed the same trend (circles).

The exact value of the ratio was dependent on experimental conditions. In the fovea low values are observed even at low temporal frequencies. In the parafovea relatively high values are observed even at moderate to high temporal frequencies. Our data show that temporal frequency has as much of an effect on the detection vs identification sensitivity ratio as eccentricity has. The curves shown in Figs 14 and 15 cover the whole range of values previously reported.

Chromatic motion as a foveal specialization

Sensitivity to isoluminant stimuli shows a remarkable decline with increasing eccentricity (Mullen, 1991; Stromeyer, Lee & Eskew, 1992b). This is confirmed in our study where there is a difference in chromatic threshold

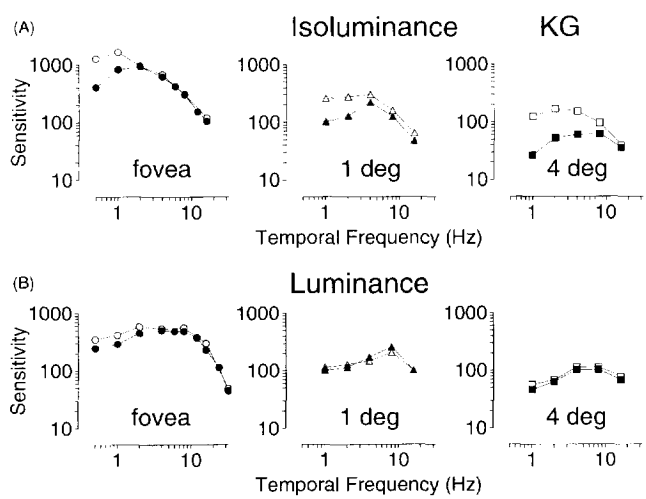

FIGURE 13. Cone contrast sensitivity for the detection (open symbols) and identification of direction of motion (solid symbols) of a 1 c/deg sinewave grating for subject KG. Left graphs are for the foveal, large field condition, middle graphs for the perifoveal condition (eccentricity 1 deg), and right graphs for the parafoveal condition (eccentricity 4 deg). (A) Isoluminance; (B) luminance.

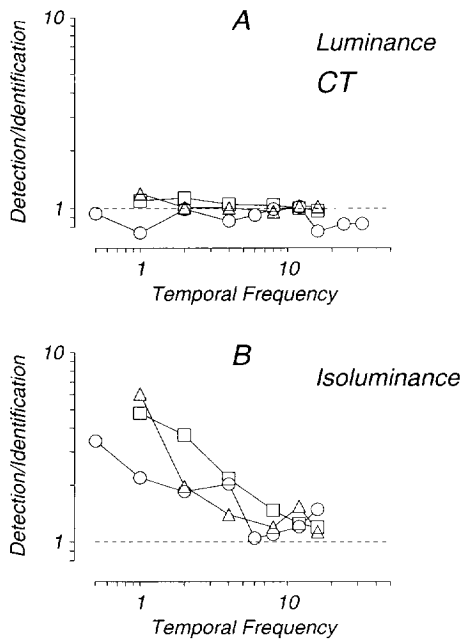

FIGURE 14. Ratios of detection vs identification sensitivities for the data from Fig. 12 for subject CT. Fovea ○; perifovea △; parafovea □. (A) Luminance, (B) isoluminance.

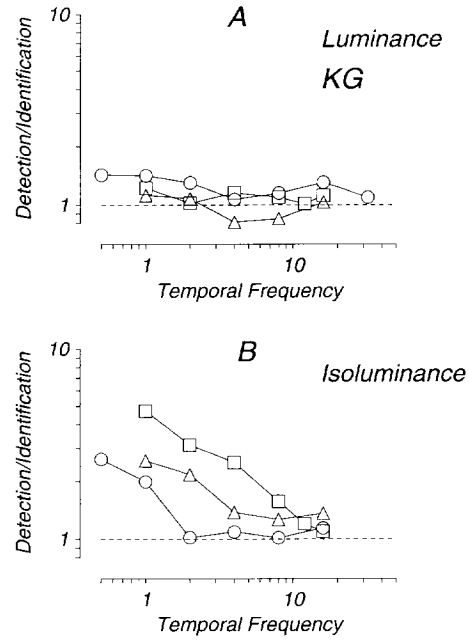

FIGURE 15. Ratios of detection vs identification sensitivities for the data from Fig. 13 for subject KG. Symbols as in Fig. 14. (A) Luminance, (B) isoluminance.

of about 1.5 log units between fovea and parafovea for slowly moving gratings. For luminance there are also differences, but they are not nearly as large. It is well established that luminance contrast sensitivity is dependent on eccentricity and declines with cortical magnification factor (Romavo, Virsu & Näsänen, 1978). The variation in chromatic sensitivity with eccentricity for moving grating patches has not been studied in detail, but there are many indications that chromatic sensitivity declines rapidly away from the fovea, just as it does for stationary gratings (Mullen, 1991). Although we cannot directly compare the absolute sensitivity between our foveal and parafoveal targets because of differences in size, target duration and temporal windowing, the comparison of relative changes are valid. The relative changes in sensitivity are the most important aspects in this study. Firstly consider the luminance targets. For the three eccentricity conditions the curves for detection and identification are almost parallel [Figs 12(A) and 13(A)], indicating a graded decrease in performance with eccentricity. Figure 16 shows sensitivity relative to the fovea for the four different conditions (luminance and isoluminance by detection and identification) at three different temporal frequencies and averaged across different observers. The most important aspects shown in Fig. 16 are that at low temporal frequencies (1) performance decreased more rapidly for isoluminance than for luminance; and (2) for isoluminance identification sensitivity falls more rapidly than detection sensitivity. At medium and high temporal frequencies there was a graded decrease in performance with eccentricity. No differences between luminance and isoluminance, or between detection and identification were observed. This indicates that the identification of slowly moving

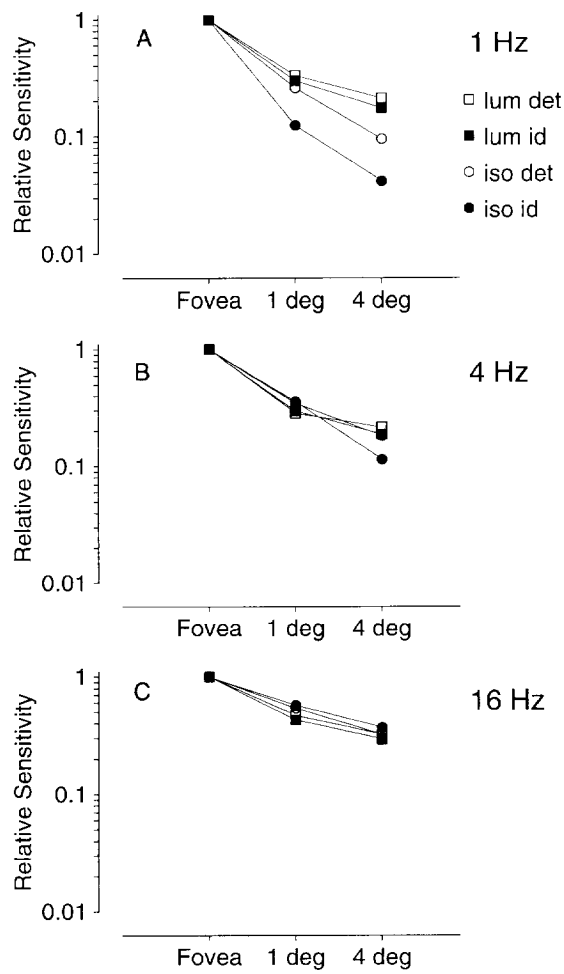

FIGURE 16. Relative sensitivities for detection and identification of luminance and isoluminant gratings at three eccentricities. Sensitivities were first averaged across the two subjects (CT and KG) and then scaled relative to performance in the fovea. (A) 1 Hz, (B) 4 Hz and (C) 16 Hz.

isoluminant gratings is undertaken by a mechanism specialized to foveal vision.

High temporal frequencies

In the preceding sections we have shown that the behavior at high temporal frequencies is different from the behavior at low temporal frequencies. When fitting models to the threshold contours there was a systematic steepening of the part of the threshold contour attributed to the luminance mechanism. This is seen in the contours for two subjects for temporal frequencies of 8, 12 and 16 Hz (Fig. 17). The contours shown are for the parafovea, contours for other eccentricities were similar. For 8 Hz and for all temporal frequencies lower than 8 Hz there were no stimuli for which thresholds fall above the bold line that indicates the luminance contrast at threshold for the black–white stimulus. At 12 and 16 Hz the situation appears to be different. The contour is steeper, a finding that is consistent for all subjects. There are several stimuli that preferentially excite the M-cones which at their threshold have a higher luminance contrast [as defined by the human photometric luminance sensitivity curve $V(\lambda)$] than required for the black–white stimulus. In fact, for most stimuli the contrast for the L-cones seems to determine threshold.

This steepening of the threshold contours is reflected in the slopes derived from the fit to the luminance mechanism. The derived slope was estimated to be -2 at low temporal frequencies, which is close to photometric isoluminance. At high temporal frequencies the slope reached values of up to -12. This indicates a clear dominance of L-cones at high temporal frequencies. This imbalance could be caused by differences in the temporal properties of the cones themselves, for example a relative phase shift between the L- and M-cones due to a temporal delay in one of the cones (Hamer & Tyler, 1992). Alternatively, different weighting functions of second-stage mechanisms for the cone inputs could cause the same type of behavior. If the imbalance is due to different temporal properties of the receptors themselves, then thresholds should not change if we use stimuli that differentially activate cone classes. Therefore we measured sensitivity to stimuli isolating the L- and the M-cones by "silent substitution". In Fig. 18 contrast for the luminance stimulus is equal to the contrast in the L- or M-cones. For the L- and M-cone isolating stimuli contrasts are specified as the contrast in the activated cone class.

The results of these experiments show that at low temporal frequencies sensitivity for the cone-isolating

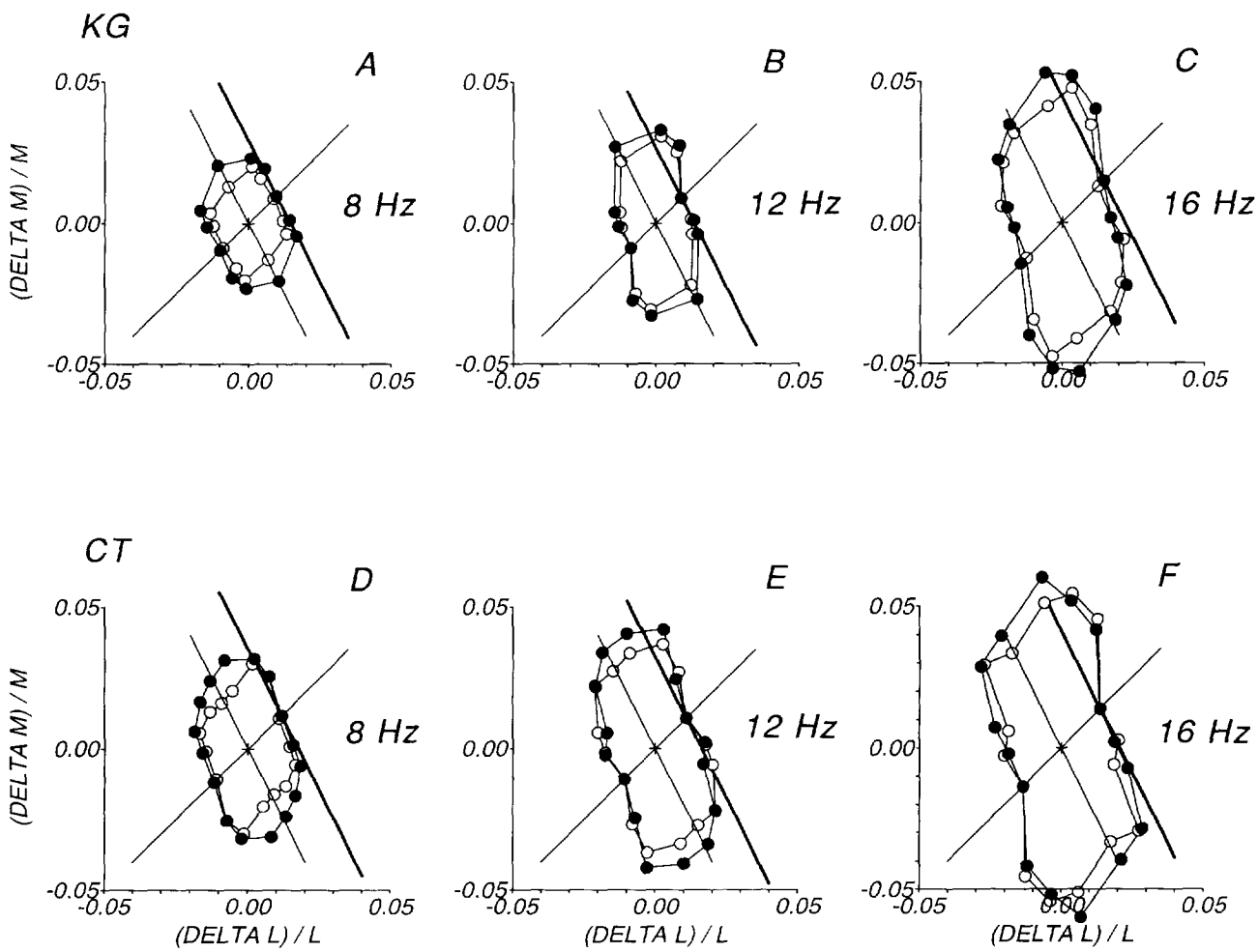

FIGURE 17. Threshold contours for subjects KG (A–C) and CT (D–F) for the parafoveal condition (eccentricity of 4 deg). The bold line shows the luminance contrast at the threshold for detecting the luminance (black–white) pattern.

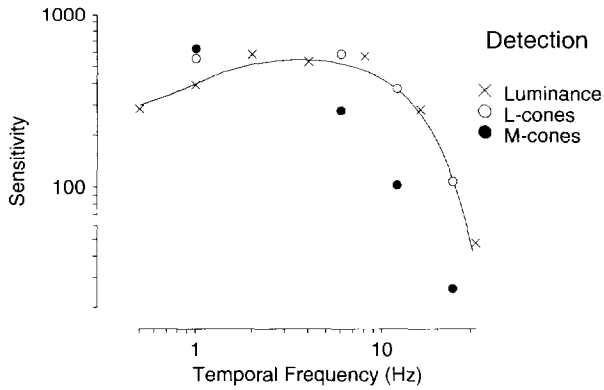

FIGURE 18. Sensitivities for the detection of a 1 Hz grating varying in luminance (×), L-cone contrast (○) or M-cone contrast (●) for subject KG. The solid curve shows the best fit of a difference-of-Gaussians to the luminance data.

stimuli is actually higher than for luminance. This apparently paradoxical result is caused by the fact that cone-isolating stimuli are "detected" by a color-opponent mechanism at low temporal frequencies, which is more sensitive to these stimuli than the luminance mechanism. Adding the two threshold-level cone-isolating stimuli in luminance peaks-add phase will therefore make the sum invisible to the observer, because the chromatic components cancel out, and the luminance mechanism is less sensitive. At high temporal frequencies sensitivity for luminance equals sensitivity to the L-cone stimulus. Similar results were obtained for the other two subjects. This is incompatible with a simple phase shift explanation. However, the results cannot discriminate between a change in the sensitivity of the photoreceptors themselves, and a change in the relative weights of the luminance mechanism for the two cone types.

DISCUSSION

We have measured the contributions of the three cone classes to the detection of moving stimuli and to the identification of their direction of motion. Our experiments show that the perception of motion is supported in all directions of color space we tested and at all eccentricities and temporal frequencies. At low temporal frequencies we found that the thresholds for detection were lower than the threshold for identification for all stimuli with the exception of the luminance direction. This difference between detection and identification threshold became more pronounced with increasing eccentricity. For foveally viewed patterns the ratio of detection to identification sensitivity was always relatively low (between 1 and 2), even though there was some variability between observers. For parafoveally viewed stimuli the ratio of detection to identification sensitivity could reach values of up to 5 (Fig. 14). In the next section we discuss the putative mechanisms that might underlie these variations in sensitivity with temporal frequency and eccentricity.

Cone contributions to motion

Our quantitative analysis of cone contributions allowed us to identify two mechanisms underlying the perception of motion. At high temporal frequencies the shape of the threshold contours is independent of eccentricity. The underlying mechanism is dominated by the L-cones and receives a weak input from S-cones. Stromeyer *et al.* (1990, 1992a) also report that identification of direction of motion is dominated by L-cones. Recently they showed that the cone contributions to a large degree depend on field color (Stromeyer, Chapparo, Tolias & Kronauer, 1994). There is an additional contribution from the S-cones at high temporal frequencies, which has been previously reported by Lee and Stromeyer (1989). They found that the S-cone signal is phase shifted 180 deg and then subtracted from the luminance signal. Our data indicate an addition of the (unshifted) S-cone signal to the L-cone signal, which gives basically the same result as a 180 deg phase shift and subtraction. Based on our data we cannot discriminate between the two possibilities. The contributions of the S-cone signal seen for luminance [L + M, Fig. 4(C)] and for blue–yellow [(L + M) − S, Fig. 5(C)] stimuli are identical in sign suggesting a common source. At low temporal frequencies our data indicate luminance and color-opponent mechanisms in accordance with the human photometric $V(\lambda)$ curve. The contribution of S-cones is negligible. In contrast to our results Lindsay and Teller (1990) found a large negative S-cone input to motion identification even at low temporal frequencies, where we do not see any contribution of S-cones. However, the average illuminances in their experiments were rather low, so that rod intrusion could have caused their results.

Motion pathways

The threshold measurements presented in this paper complement our recent results on speed judgments of suprathreshold stimuli. The speed judgment measurements show that the perceived speed is contrast dependent only at low temporal frequencies, and that the contrast dependence is quite different for luminance and isoluminant stimuli. At high temporal frequencies speed judgments are invariant to changes in contrast or chromaticity (Hawken *et al.*, 1994). Our conclusion was that motion processing is fundamentally different at low and high temporal frequencies.

In our current experiments there is no difference between detection and identification thresholds at high temporal frequencies for either luminance or chromatic stimuli. In addition, the same "fast" mechanism seems to be evident in the fovea and in parafovea. This mechanism has some residual sensitivity for isoluminant stimuli, both red–green and blue–yellow. At low temporal frequencies there are distinct thresholds for detection and identification for stimuli near isoluminance, while for achromatic stimuli the thresholds are the same. In addition, for low temporal frequencies there are differences in the ratio of detection to identification threshold with eccentricity

which is unlike the behavior observed at high temporal frequencies. One interpretation of these results is that separate mechanisms are responsible for signaling the direction of motion of luminance and chromatic borders at low temporal frequencies.

The substrate for the "fast" mechanism is likely to include the magnocellular pathway via the cortical areas V1 and MT. The main concentration of directionally selective cells in the output layers of V1 is in layers 4B and 6 (Hubel & Wiesel, 1968; Dow, 1974; Livingstone & Hubel, 1984; Orban, Kennedy & Bullier, 1986; Hawken, Parker & Lund, 1988). Some of these direction selective cells receive a dominant input from the magnocellular pathway, indicated by the finding that they show a distinct null in their responses at photometric isoluminance (Hawken, Shapley & Grosof, 1993). Layers 4B and 6 in V1 have a direct projection to MT (Shipp & Zeki, 1985; Fries, Keizer & Kuypers, 1985). Although some MT neurons show responses to isoluminant stimuli (Saito, Tanaka, Isono, Yasuda & Mikami, 1989; Charles & Logothetis, 1989; Dobkins & Albright, 1990; Gegenfurtner, Kiper, Beusmans, Carandini, Zaidi & Movshon, 1994) these responses are mostly due to variations in the individual cells' isoluminant point (Gegenfurtner *et al.*, 1994). More importantly, Gegenfurtner *et al.* (1994) reported that neuronal and psychophysical sensitivity for isoluminant stimuli are only matched at high temporal frequencies.

Monkey observers from the study of Gegenfurtner *et al.* (1994) and human observers in this study showed similar detection performance for chromatic stimuli at low temporal frequencies. The psychophysically determined sensitivity of the monkey observer to low temporal frequency isoluminant stimuli is much higher than the sensitivity of MT cells (Gegenfurtner *et al.*, 1994). Therefore MT is unlikely to underlie the perception of slowly moving isoluminant gratings. Logothetis and Charles (1990) have already shown that some V4 cells are selective both to color and direction of motion, and Gegenfurtner, Kiper and Fenstemaker (1993) have shown that a significant interaction between color and motion already takes place in area V2 of macaques. The current evidence implies two separate motion systems, one for low temporal frequencies, that is sensitive to color, and another for high temporal frequencies, that is mostly sensitive to luminance and whose psychophysical properties closely match the behavior of MT cells.

REFERENCES

Cavanagh, P. & Anstis, S. (1991). The contribution of color to motion in normal and color-deficient observers. *Vision Research*, *31*, 2109–2148.

Cavanagh, P. & Favreau, O. E. (1985). Color and luminance share a common motion pathway. *Vision Research*, *25*, 1595–1601.

Cavanagh, P., Tyler, C. W. & Favreau, O. (1984). Perceived velocity of moving chromatic gratings. *Journal of the Optical Society of America A*, *1*, 893–899.

Charles, E. R. & Logothetis, N. K. (1989). The responses of middle-temporal (MT) neurons to isoluminant stimuli. *Investigative Ophthalmology and Visual Science (Suppl.)*, *30*, 427.

Derrington, A. M. & Badcock, D. R. (1985). The low level motion system has both chromatic and luminance inputs. *Vision Research*, *25*, 1874–1884.

Derrington, A. M. & Henning, G. B. (1993). Detecting and discriminating the direction of motion of luminance and colour gratings. *Vision Research*, *33*, 799–811.

Derrington, A. M., Krauskopf, J. & Lennie, P. (1984). Chromatic mechanisms in lateral geniculate nucleus of macaque. *Journal of Physiology*, *357*, 241–265.

Dobkins, K. R. & Albright, T. D. (1990). Color facilitates motion correspondence in visual area MT. *Society of Neuroscience Abstracts*, *16*, 1220.

Dow, B. M. (1974). Functional classes of cells and their laminar distribution in monkey visual cortex. *Journal of Neurophysiology*, *37*, 927–946.

Fries, W., Keizer, K. & Kuypers, H. G. J. M. (1985). Layer V1 cells in macaque striate cortex project to both superior colliculus and prestriate visual area V5. *Experimental Brain Research*, *58*, 613–616.

Gegenfurtner, K. R. & Hawken, M. J. (1992). Cone contributions to motion detection and identification. *Optical Society of America Technical Digest*, *23*, 62.

Gegenfurtner, K. R. & Hawken, M. J. (1993). Temporal and chromatic properties of motion mechanisms. *Investigative Ophthalmology and Visual Science (Suppl.)*, *34*, 743.

Gegenfurtner, K. R., Kiper, D. C. & Fenstemaker, S. B. (1993). Chromatic properties of neurons in macaque V2. *Society for Neuroscience Abstracts*, *19*, 769.

Gegenfurtner, K. R., Kiper, D. C., Beusmans, J., Carandini, M., Zaidi, Q. & Movshon J. A. (1994). Chromatic properties of neurons in Macaque MT. *Visual Neuroscience*, *11*, 455–466.

Gorea, A., Papathomas, T. V. & Kovacs, I. (1993). Motion perception with spatiotemporally matched chromatic and achromatic information reveals a "slow" and a "fast" motion system. *Vision Research*, *33*, 2515–2534.

Hamer, R. D. & Tyler, C. W. (1992). Analysis of visual modulation sensitivity—V. Faster visual response for G- than for R-cone pathway. *Journal of the Optical Society of America A*, *9*, 1889–1904.

Hawken, M. J., Gegenfurtner, K. R. & Tang, C. (1994). Contrast dependence of colour and luminance motion mechanisms in human vision. *Nature*, *367*, 268–270.

Hawken, M. J., Parker, A. J. & Lund, J. S. (1988). Laminar organization and contrast sensitivity of direction-selective cells in the striate cortex of the Old World Monkey. *Journal of Neuroscience*, *8*, 3541–3548.

Hawken, M. J., Shapley, R. M. & Grosof, D. H. (1993). Organization of chromatic inputs to direction selective neurons in macaque V1. *Investigative Ophthalmology and Visual Science (Suppl.)*, *34*, 460.

Hess, R. H., Baker C. L. Jr & Zihl, J. (1989). The "motion-blind" patient: Low level spatial and temporal filters. *Journal of Neuroscience*, *9*, 1628–1640.

Hubel, D. H. & Wiesel, T. N. (1968). Receptive fields and functional architecture of monkey striate cortex. *Journal of Physiology*, *195*, 215–243.

Krauskopf, J., Williams, D. R. & Heeley, D. W. (1982). Cardinal directions of color space. *Vision Research*, *22*, 1123–1131.

Lee, J. & Stromeyer, C. F. III (1989). Contribution of human short-wave cones to luminance and motion detection. *Journal of Physiology*, *413*, 563–593.

Lindsey, D. T. & Teller, D. Y. (1990). Motion at isoluminance: Discrimination/detection ratios for moving isoluminant gratings. *Vision Research*, *30*, 1751–1761.

Livingstone, M. S. & Hubel, D. H. (1984). Anatomy and physiology of a color system in the primate visual cortex. *Journal of Neuroscience*, *4*, 309–356.

Livingstone, M. S. & Hubel, D. H. (1987). Psychophysical evidence for separate channels for the perception of form, color, movement, and depth. *Journal of Neuroscience*, *7*, 3416–3468.

Logothetis, N. K. & Charles, E. R. (1990). V4 responses to gratings

defined by random dot motion. *Investigative Ophthalmology and Visual Science (Suppl.)*, *31*, 90.

MacLeod, D. I. A. & Boynton, R. M. (1979). Chromaticity diagram showing cone excitation by stimuli of equal luminance. *Journal of the Optical Society of America*, *69*, 1183–1186.

Maloney, L. T. & Knoblauch, K. (1994). Identifying color mechanisms from chromatic discrimination data by analysis of residuals. *Perception*, *23*, 94–95.

Merigan, W. H., Byrne, C. E. & Maunsell, J. H. R. (1991). Does primate motion perception depend on the magnocellular pathway? *Journal of Neuroscience*, *11*, 3422–3429.

Metha, A. B., Vingrys, A. J. & Badcock, D. R. (1994). Detection and discrimination of moving stimuli: The effects of color, luminance, and eccentricity. *Journal of the Optical Society of America A*, *11*, 1697–1709.

Mullen, K. T. (1991). Colour vision as a post-receptoral specialization of the central visual field. *Vision Research*, *31*, 119 130.

Mullen, K. T. & Baker, C. L. Jr (1985). A motion aftereffect from an isoluminant stimulus. *Vision Research*, *25*, 685–688.

Mullen, K. T. & Boulton, J. C. (1992). Absence of smooth motion perception in color vision. *Vision Research*, *32*, 483–488.

Nielson, K. R. K. & Wandell, B. A. (1988). Discrete analysis of spatial-sensitivity models. *Journal of the Optical Society of America A*, *5*, 743–755.

Orban, G. A., Kennedy, H. & Bullier, J. (1986). Velocity sensitivity and direction selectivity of neurons in areas V1 and V2 of the monkey: Influence of eccentricity. *Journal of Neurophysiology*, *56*, 462–480.

Palmer, J., Mobley, L. A. & Teller, D. Y. (1993). Motion at isoluminance: Discrimination/detection ratios and the summation of luminance and chromatic signals. *Journal of the Optical Society of America A*, *10*, 1353–1362.

Poirson, A. B., Wandell, B. A., Varner, D. C. & Brainard, D. H. (1990). Surface characterization of color thresholds. *Journal of the Optical Society of America A*, *7*, 783–789.

Ramachandran, V. S. & Gregory, R. L. (1978). Does color provide an input to human motion perception. *Nature*, *275*, 55–56.

Romavo, J., Virsu, V. & Näsänen, R. (1978). Cortical magnification factor predicts the photopic contrast sensitivity of peripheral vision. *Nature*, *271*, 54–56.

Saito, H., Tanaka, K., Isono, H., Yasuda, M. & Mikami, A. (1989). Directionally selective response of cells in the middle temporal area (MT) of the macaque monkey to movement of equiluminous opponent color stimuli. *Experimental Brain Research*, *75*, 1–14.

Shipp, S. & Zeki, S. M. (1985). Segregated output to area V5 from layer 4b of macaque monkey striate cortex. *Journal of Physiology*, *369*, 32P.

Smith, V. C. & Pokorny, J. (1975). Spectral sensitivity of the foveal cone photopigments between 400 and 500 nm. *Vision Research*, *15*, 161–171.

Stone, L. S. & Thompson, P. (1992). Human speed perception is contrast dependent. *Vision Research*, *32*, 1535–1549.

Stromeyer, C. F. III, Eskew, R. T. & Kronauer, R. E. (1990). The most sensitive motion detectors in humans are spectrally-opponent. *Investigative Ophthalmology and Visual Science (Suppl.)*, *31*, 240.

Stromeyer, C. F. III, Kronauer, R. E. & Eskew, R. T. (1992a). Relative temporal phase of L and M cone signals within the luminance motion pathway. *Investigative Ophthalmology and Visual Science (Suppl.)*, *33*, 756.

Stromeyer, C. F. III, Lee, J. & Eskew, R. T. (1992b). Peripheral chromatic sensitivity for flashes: A post-receptoral red–green asymmetry. *Vision Research*, *32*, 1865–1873.

Stromeyer, C. F. III, Chapparo, A., Tolias, A. S. & Kronauer, R. E. (1994). Colored fields produce large L vs M phase shifts in luminance motion mechanism. *Investigative Ophthalmology and Visual Science (Suppl.)*, *35*, 1644.

Stromeyer, C. F. III, Kronauer, R. E., Ryu, A., Chaparro, A. & Eskew, R. T. (1995). Contributions of human long-wave and middle-wave cones to motion detection. *Journal of Physiology*. In press.

Thompson, P. (1982). Perceived rate of movement depends on contrast. *Vision Research*, *22*, 377–380.

Watson, A. B., Thompson, P. G., Murphy, B. J. & Nachmias, J. (1980). Summation and discrimination of gratings moving in opposite directions. *Vision Research*, *20*, 341–347.

Zeki, S. M. (1978). Uniformity and diversity of structure and function in rhesus monkey prestriate visual cortex. *Journal of Physiology*, *277*, 273–290.

Zihl, J., Von Cramon, D. & Mai, N. (1983). Selective disturbance of movement vision after bilateral brain damage. *Brain*, *106*, 313–340.

Acknowledgements—We would like to thank Walt Kropfl for extending our Vista board to allow for a higher color resolution and John Krauskopf for letting us run some of the experiments in his laboratory. John Krauskopf and Karl-Heinz Bäuml kindly commented on the manuscript. We also would like to thank Andrew Derrington and Charles Stromeyer III for their critical reviews. The experiments were performed while K. R. G. was a postdoctoral fellow in J. A. Movshon's laboratory at NYU and was supported by Howard Hughes Medical Institute. Supported by NEI grant EY08300 to M.J.H.